J. Nano- Electron. Phys.
3 (2011) No1, P. 1035-1040

© 2011 SumDU
(Sumy State University)

PACS numbers: 81.07.De, 73.22. – f, 71.15.Mb, 71.20.Nr

VACANCY DEFECT RECONSTRUCTION AND ITS EFFECT ON ELECTRON TRANSPORT IN SI-C NANOTUBES

S. Choudhary*, S. Qureshi#

IIT Kanpur,
Department of Electrical Engg., Kanpur, India
E-mail: *suds@iitk.ac.in, #qureshi@iitk.ac.in

We investigate the vacancy defect reconstruction and its effect on I-V characteristics in a (4, 0) *zigzag and* (5, 5) *armchair silicon-carbide nanotubes* (SiCNTs) *by applying self consistent non-equilibrium Green's function formalism in combination with the density-functional theory to a two probe molecular junction constructed from* SiCNTs. *The results show that single vacancies and di-vacancies in* SiCNTs *have different reconstructions. A single vacancy when optimized, reconstructs into a* 5-1DB *configuration in both zigzag and armchair* SiCNTs, *and a di-vacancy reconstructs into a* 5-8-5 *configuration in zigzag and into a* 5-2DB *configuration in armchair* SiCNTs. *Introduction of vacancy increases the band gap of* (4, 0) *metallic* SiCNT *and decreases the bandgap of* (5, 5) *semiconducting* SiCNT, *bias voltage dependent current characteristic show reduction in overall current in metallic* SiCNT *and an increase in overall current in semiconducting* SiCNT.

Keywords: *NANOTUBE, SiCNT, ARMCHAIR-ZIGZAG, DEFECTS, VACANCY.*

(Received 04 February 2011)

1. INTRODUCTION

The high energy difference between the *sp*2 and *sp*3 bonds (1.25 eV per Si-C pair) [1], which makes the existence of a silicon carbide (SiC) graphitic phase impossible, has not obstructed the scientists from synthesizing SiC nanotubes (SiCNTs) [2] [3]. Recently, the scientists have suggested to make silicon carbide nanotubes (SiCNTs) as a possible alternative to carbon nanotubes (CNTs) for field emitting applications [2] [3], which has boosted the interest for SiCNTs and several studies on the electronic properties of SiCNTs can be found in the literature [4-7]. Vacancy reconstruction is well known for CNTs [8-9], band gap of semiconducting CNT reduces and conducting CNT increases when a vacancy is introduced [10]. Therefore, it is of interest to understand how the vacancy reconstruction takes place in SiCNTs and what its effect on electron transport properties is.

In the process of the growth of CNTs or SiCNTs, a variety of structural defects inevitably occur, which can affect their electronic properties. Vacancies are the most common defects in CNTs, and have drawn much research attention in recent years [8] [11-12]. An ideal single vacancy containing three hanging bonds is unstable [8], two of the three dangling bonds form a new C–C bond and the structure becomes a pentagonal ring coupled with one dangling bond, which forms a so-called 5-1DB defect [8] [11] [13]. The reconstruction of di-vacancy in CNTs results into an octagonal ring coupled to two pentagonal rings [8] [13], the new 5-8-5 structure does

not have a hanging bond. Another study [10], suggests that an introduction of vacancy on single wall carbon nanotubes (SWCNTs) can have a large impact on electronic properties, vacancy reconstruction and its effects on electronic properties in SiCNTs is still an open question.

In the present work, we investigate the single and di-vacancy reconstruction in (4, 0) and (5, 5) SiCNTs by using steepest descent method of geometry optimization. Electronic properties of optimized structures were also investigated by studying the transmission energy spectrum $T(E)$, density of states (*DOS*) and current-voltage (*I-V*) characteristics. The calculations were carried out on an *ab initio* based simulator called Atomistix [14] which uses density functional theory (DFT) and non equilibrium Green's functions formulations (NEGF) together for obtaining electronic transport properties of molecules and devices. More details about the method and software could be found in previous reports [15-17].

2. SIMULATION SETUP AND VACANCY RECONSTRUCTION RESULTS

A perfect (no defects) (4, 0) and (5, 5) SiCNTs are shown in Fig. 1, SiCNT structures with single and di-vacancy defects are also shown, Si-C bond length of 1.78 Å [3] [7] and 1:1 Si-C ratio was considered. A two probe geometry [18] that consists of a left electrode, right electrode and a central region (scattering region) was constructed.

For studying vacancy reconstruction, the whole setup was optimized (electrodes fixed) using steepest descent method of geometry optimization. In the case of (4, 0) zig-zag SiCNT, a single vacancy reconstructs into 5-1DB defect similar to that in CNTs [11], here two of the three dangling bonds (marked as 2 and 3 in Fig. 1a) form a new Si-Si bond (2.36 Å bond length) and the structure becomes a pentagonal ring coupled with one dangling bond. The reconstruction of di-vacancy in (4, 0) SiCNT is also similar to that in CNTs [8] [13], here the reconstruction results into an octagonal ring coupled to two pentagonal rings (see Fig. 1a), the new 5-8-5 structure has a C-C and Si-Si bond, it does not have a hanging bond.

In the case of (5, 5) armchair SiCNT, a single vacancy reconstructs into 5-1DB defect similar to that in (4, 0) SiCNT and CNTs [11]. However, the reconstruction of a di-vacancy forms a new 5-2DB defect in (5, 5) armchair SiCNT, two of the four dangling bonds (marked as 3 and 4 in Fig. 1b) form a new C–C bond and the structure becomes a pentagonal ring coupled with two dangling bonds (marked as 1 and 2 in Fig. 1b). The separation width between these two Si atoms associated with hanging bonds is 2.55 Å.

The electron transport characteristic of a SiCNT may depend on its length, resistance, contacts and applied bias. We neglect length dependency by considering a minimal length segment of nanotube in the central region. In order to minimize the contact dependency, SiCNT electrodes similar to the central region were used to construct two probe system. The lengths of the central regions, screening layers and the electrodes of the simulated sections were taken as 8 periods (32 C atoms and 32 Si atoms), 2 periods (8 C atoms and 8 Si atoms) and 2 periods (8 C atoms and 8 Si atoms), for (4, 0) SiCNT. In case of (5, 5) SiCNT, central region was 4 periods (40 C and 40 Si atoms), screening layers and electrodes were taken as one period each (20 C and 20 Si atoms). Hence, a central region width (SiCNT length) of 22.25 Å for (4, 0) and 13.87 Å for (5, 5) SiCNT were used in the simulation.

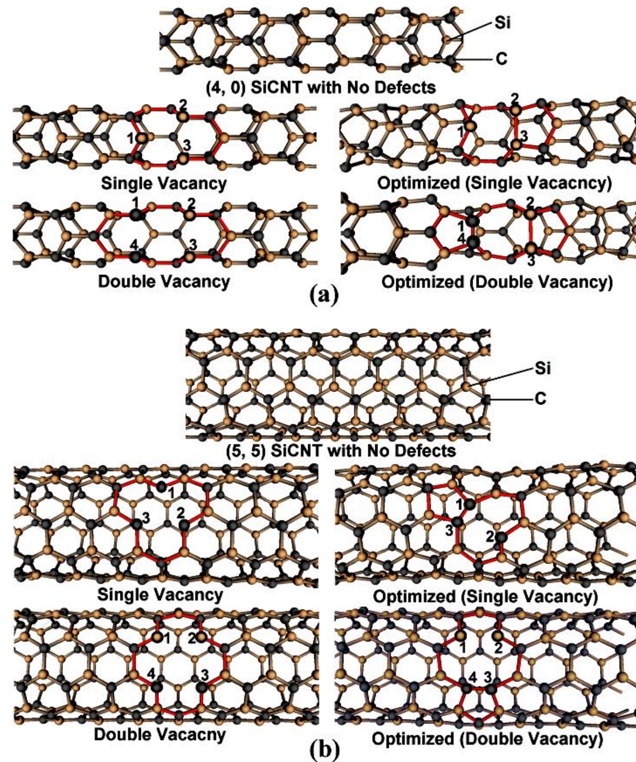

Fig. 1 – (*a*) 5-1DB *defect in single vacancy optimization of* (4, 0) *zig-zag* SiCNT *and* (*b*) 5-2DB *defect in di-vacancy optimization of* (5, 5) *armchair* SiCNT

The simulation parameters were selected to provide accurate measurements as reported for CNTs [18] and are following: mesh cut-off energy was 400 Ry, basis set was double zeta polarized with 0.001 Bohr radial sampling, exchange correlation functional was set to local density approximation (LDA) type with double zeta polarized (DZP) basis set, Brillouin zone integration parameters of electrodes are taken as (1, 1, 500). Electrode temperature was set to 1000 K which makes the convergence easier; it has no effect on the overall measurement which was also verified at lower electrode temperatures. Due to the requirement of heavy computing resources, we used the above parameters which shall ensure simulation convergence.

3. ELECTRON TRANSPORT RESULTS AND ANALYSIS

Simulation results are presented in Fig. 2, where *I-V* characteristic is shown and in Fig. 3, where zero bias transmission energy spectrum $T(E)$ and density of states *DOS* results are shown. Let us first look at the bias voltage dependent current of Fig. 2, a (4, 0) SiCNT is metallic by nature [4] [6], small reduction in current can be observed for both single and di-vacancy defects. This is due to a small increase in band gap in vacancy defected metallic SiCNTs (band gap with no defect is 0 eV and with double vacancy is 0.074 eV for bulk system, see Fig. 4a), an increase in bandgap was also reported in case of metallic CNTs in the literature [10]. However, introduction of vacancy

reduces the bandgap of semiconducting (5, 5) SiCNT (band gap with no defect is 1.91 eV and with double vacancy is 0.203 eV for bulk system, see Fig. 4b), similar to bandgap reduction in semiconducting CNTs [10], which results in a large increase in current in semiconducting SiCNTs (see Fig. 2b). The band gap for bulk system was calculated from the energy band plot similar to Fig. 4, by extracting the HOMO (Highest Occupied Molecular Orbital) and LUMO (Lowest Unoccupied Molecular Orbital) bands (i.e. the lowest conduction band and highest valence band) and taking the difference in all k-points and selecting the smallest value.

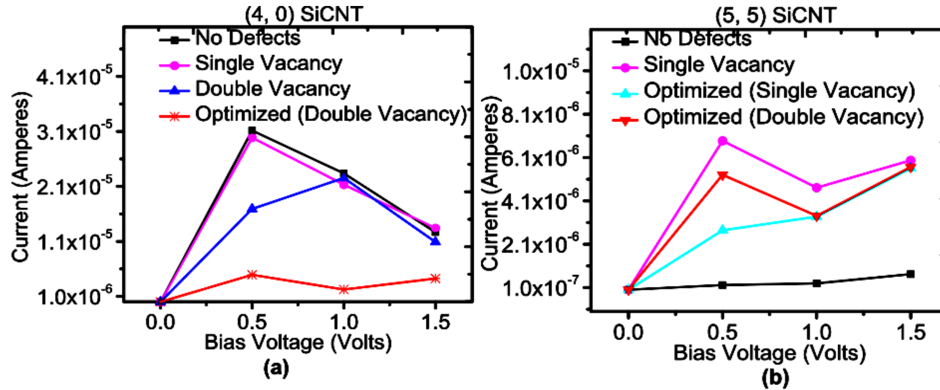

Fig. 2 – *Bias voltage dependent current characteristic* (*I-V characteristic*) *of* (4, 0) *and* (5, 5) SiCNT *two probe system. Current is shown to vary in perfect and vacancy defected* SiCNTs

To gain more insight of *I-V* characteristic, we study $T(E)$ and *DOS* results of the ideal and deformed SiCNTs, and compare them. The transmission spectrum describes the probability for electron with incident energy E to transfer from the left electrode to the right electrode and the integral of the transmission spectrum yields the current through the system [15]. The equation for calculating current from the transmission spectrum can be found in literature [15].

The equilibrium transport properties (no bias voltage applied) of the two-probe model were investigated firstly. $T(E)$ at zero-bias (equilibrium transport) is shown in Fig. 3 by black curve, here the Fermi energy is set as 0 eV [15], *DOS* is shown by red curve. $T(E)$ of (4, 0) SiCNT in Fig. 3a, reflects the conducting nature of SiCNT with a finite transmission around 0 eV (Fermi level), which is also confirmed by the overlapping of HOMO and LUMO bands in energy band plot of Fig. 4a. The semiconducting nature of (5, 5) SiCNT is confirmed by a wide transmission gap seen as a flat curve around 0 eV in Fig. 3b and also by inspecting the energy band plot where a band gap of 1.91 eV could be observed. The *I-V* characteristic of metallic (4, 0) SiCNT is in confirmation with $T(E)$ and *DOS* results. Bandgap of metallic (4, 0) SiCNT increases with the introduction of vacancy (see Fig. 4b), which results in an increase in transmission gap (see Fig. 3a) and a reduction in current (see Fig. 2a). In the case of (5, 5) semiconducting SiCNT, introduction of vacancy reduces the bandgap (see Fig. 4b) resulting in increase in current, which is also confirmed by the reduction in transmission gap around Fermi level (see Fig. 3b).

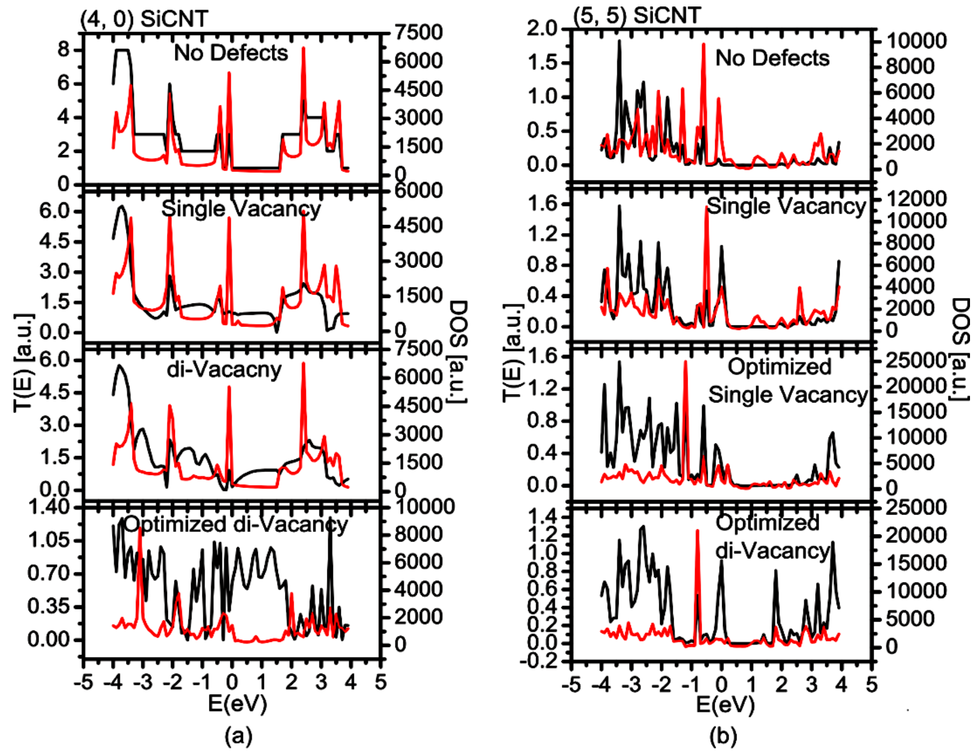

Fig. 3 *– Zero bias transmission spectra T(E) and density of states DOS profile of* (*a*) (4, 0) SiCNT *and* (*b*) (5, 5) SiCNT. *DOS is number of electrons/energy, i.e. unit* 1/*eV*. [*Note: a.u. is arbitrary units and E is energy in electron volts*]

We have shown energy band plot of only di-vacancy defect in Fig 4, the band gap with single vacancy defect and with geometry optimization was calculated separately from their respective energy band plots.

4. CONCLUSION

In summary, the results show that reconstruction of di-vacancy in armchair SiCNT forms a 5-2DB defect, which is different from the reconstruction of CNTs and zig-zag SiCNT. Vacancy introduction reduces the bandgap of semiconducting SiCNTs and increases the bandgap of conducting SiCNTs (converts them to semi-metallic nanotubes), which results in large increase in current in semiconducting SiCNTs and a small reduction in current in conducting SiCNTs, respectively.

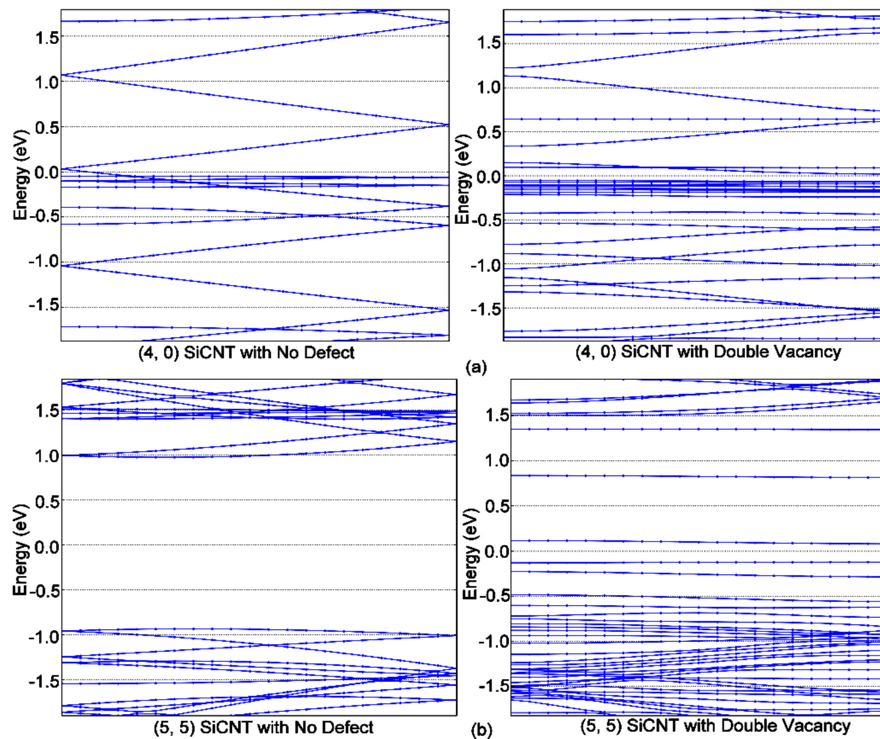

Fig. 4 *– Energy band [k-point, energy] plot of (a) zig-zag* (4, 0) SiCNT *and (b) armchair* (5, 5) SiCNT *with no defect and with di-vacancy defect*

REFERENCES

1. Y. Miyamoto, B.D. Yu, *Appl. Phys. Lett.* **80,** 586 (2002).
2. T. Taguchia, N. Igawaa, H. Yamamotoa, S. Shamotoa, S. Jitsukawa, *Physica E* **28,** 431 (2005).
3. G. Alfieri, T. Kimoto, *Appl. Phys. Lett.* 97, 043108 (2010).
4. I.J. Wu, G.Y. Guo, *Phys. Rev. B.* **76,** 035343 (2007).
5. M. Zhao, Y. Xia, F. Li, R.Q. Zhang, S.T. Lee, *Phys. Rev. B.* **71,** 085312 (2005).
6. E.V. Larina, V.I. Chmyrev, V.M. Skorikov, P.N. Dyachkov, D.V. Makaev, *Inorg. Mater.* **44,** 823 (2008).
7. Z. Wang, X. Zu, H. Xiao, F. Gao, W.J. Weber, *Appl. Phys. Lett.* **92,** 183116 (2008).
8. J. Yuan, K.M. Liew, *Carbon* **47,** 1526 (2009).
9. Z. Zanolli and J.C. Charlier, *Phys. Rev. B.* **81,** 165406 (2010).
10. L. Vincent Liu, W.Q. Tian, Y.A. Wang, *Int. J. Quant. Chem.* **109,** 3441 (2009).
11. A.J. Lu and B.C. Pan, *Phys. Rev. Lett.* **92,**105504 (2004).
12. J. Rossato, R.J. Baierle, A. Fazzio, R. Mota, *Nano. Lett.* **5,** 197 (2005).
13. P.M. Ajayan, V. Ravikumar, and J.C. Charlier, *Phys. Rev. Lett.* **81,** 1437 (1998).
14. Atomistix, *QuantumWise A/S* (www.quantumwise.com).
15. M. Brandbyge, J.L. Mozos, P. Ordejyn, J. Taylor, K. Stokbro, *Phys. Rev. B.* **65,** 165401 (2002).
16. J. Taylor, H. Guo, J. Wang, *Phys. Rev. B.* **63,** 245407 (2001).
17. J.M. Soler, E. Artacho, J.D. Gale, A. Garcia, J. Junquera, P. Ordejyn, D. Sanchez-Portal, *J. Phys.: Condens. Matter.* **14,** 2745 (2002).
18. S. Yamacli, M. Avci, *Phys. Lett. A.* **374,** 297 (2009).